Published in final edited form as:
J Neuropathol Exp Neurol. 2008 August ; 67(8): 773–783. doi:10.1097/NEN.0b013e318180ec47.

Relationships Between Expression of Apolipoprotein E and β-Amyloid Precursor Protein Are Altered in Proximity to Alzheimer β-Amyloid Plaques: Potential Explanations from Cell Culture Studies

Steven W. Barger, PhD[1,2,3], **K. Mark DeWall, PhD**[1], **Ling Liu, MD**[1], **Robert E. Mrak, MD, PhD**[2,4,5], and **W. Sue T. Griffin, PhD**[1,2,3]

[1]Department of Geriatrics, University of Arkansas for Medical Sciences, Little Rock, Arkansas

[2]Department of Neurobiology & Developmental Sciences, University of Arkansas for Medical Sciences; Little Rock, Arkansas

[3]Geriatric Research Education and Clinical Center, Central Arkansas Veterans Healthcare System, Little Rock, Arkansas

[4]Department of Pathology, University of Arkansas for Medical Sciences, Little Rock, Arkansas

Abstract

Theories about the initiation and progression of Alzheimer disease (AD) often consider potential roles played by elevations of β-amyloid precursor protein (βAPP). Since it is the source of amyloid β-peptide (Aβ), βAPP may simply contribute more pathogenic stimulus when elevated; some analyses have, however, reported a decline of βAPP in AD. We found a progressive increase in neuronal βAPP expression with increasing age in the brains of non-demented individuals, whereas in AD patient samples βAPP antigenicity decreased in neuronal somata in a manner that correlated with accumulation of mature Aβ plaques. By contrast, apolipoprotein E (ApoE) expression correlated with accumulation of plaques and even greater amounts of ApoE were detected in plaques. Induction of βAPP by glutamate in neuronal cell cultures was found to depend upon ApoE levels or activity. Thus, elevations in expression of ApoE and βAPP by cellular stresses are likely normally linked in vivo and uncoupling of this link, or other pathologic events in AD initiation, may leave neurons with diminished βAPP expression, which might in turn reduce their resistance to stressors.

Keywords

Alzheimer; Amyloid β-peptide; Apolipoprotein E; Glutamate; Immunofluorescence; RNA interference

Introduction

β-Amyloid precursor protein (βAPP) is a component of acute-phase responses to injury that has been preserved across eons of evolution (1), apparently because of its beneficial role in coping with cellular injury and stress. βAPP-knockout mice show age-related deficits in

Correspondence and reprint requests to: W. Sue T. Griffin, PhD; Reynolds Inst. on Aging, Univ. Arkansas Med. Sci.; 629 Jack Stephens Dr., Rm 3103; Little Rock, AR 72205. Tel: 501-526-5800; Fax: 501-526-5830; griffinsuet@uams.edu.
[5]Current affiliation: Department of Pathology, University of Toledo College of Medicine, Toledo Ohio

long-term potentiation and in memory-related behavior (2). Moreover, elevation of βAPP expression can be neuroprotective *in vivo* (3). The importance of βAPP in Alzheimer disease (AD) is indicated by its genetic, biochemical and neuropathological connections to the disease. In cases of trisomy of chromosome 21 AD occurs universally and the elevation of gene dosage for βAPP apparently contributes to the development of AD-related neuropathology (4,5). Several familial AD lineages have now been identified in which a more restricted duplication results in a 50% increase in gene dosage for βAPP gene, strongly suggesting that duplication of the βAPP gene alone is sufficient to cause amyloid deposition and related dementia (6,7). Nonetheless, some reports of mRNA or protein measurements show no overall elevation of βAPP in homogenates from AD brain (8,9), and some have even reported a decrease (10,11).

Apolipoprotein E is also connected to AD genetically, biochemically, and neuropathologically and it has several points of interaction with βAPP. In humans, single nucleotide polymorphisms in the coding region of the ApoE gene (*APOE*) form 3 alleles (ε2, ε3, ε4) that translate into 3 distinct protein sequences. Possession of the ε4 allele is the single most robust genetic risk factor yet identified for development of sporadic AD (12). Individuals with 2 copies of the ε4 allele of *APOE* have a 50% to 90% chance of developing AD by the age of 85 and those with one copy have an approximately 45% chance. Although the mechanism for this genetic effect remains a mystery, there are data suggesting that abnormalities can result from an increase in the absolute level of ApoE of any allelic sequence. In particular, ApoE is found in the amyloid plaques of AD (13–15) and in the deposits of amyloid β-peptide (Aβ) that occur in mouse models of the disease (16); ApoE promotes the formation of Aβ fibrils in vitro (17); indeed, ApoE is *necessary* for the accumulation of amyloid β-peptide (Aβ) deposits in mouse models of AD (16). ApoE also disrupts cytoskeletal structure and function (18) and it influences the phosphorylation of tau and the formation of neurofibrillary tangles (13,19–22). ApoE elevation has also been documented in other types of brain injury (23,24).

Although aging and other conditions of stress elevate levels of both βAPP and ApoE, a mechanistic relationship between the induction of these genes has not been documented. In this study, we found that in cognitively intact adult brains, βAPP accumulated with age but in AD brain samples, the protein is not elevated in neurons adjacent to mature plaques. In fact, these neurons show dramatically lower levels of βAPP than those remote from plaques. In neuron cell cultures, we found that interfering with ApoE expression blocked induction of βAPP by glutamatergic stress. Thus, while early events in the development of AD pathology manifest in proximity to Aβ deposits, lack of βAPP expression near plaques reflects a reversal of the tendency of βAPP levels to rise in conditions of stress, possibly resulting from interruption of a glutamate→ApoE→βAPP axis.

Materials and Methods

Subject Population

Details of subject characteristics are provided in Table 1. Tissue was obtained at autopsy from hippocampus, amygdala, and parahippocampal cortex. Individuals were characterized for ApoE genotype by restriction-digest analysis of PCR amplimers (25) or by direct sequencing. The diagnosis of AD was made according to NIH-Reagan guidelines (26), which incorporate CERAD evaluation of neuritic-plaque density (27), and Braak & Braak staging of neurofibrillary tangles (28). For mRNA comparisons, non-demented, age-matched controls (n = 5) were selected to match the AD cases closely with respect to mRNA integrity. Another cohort (“high-pathology controls”; n = 3) consisted of samples from patients that were not clinically demented but exhibited neuropathologic findings consistent with the diagnosis of AD. At autopsy, the right half of each brain was immersion-fixed in

formalin for histology and immunofluorescence. When utilized, unfixed tissue was obtained from the left half of the brain, dissected fresh into various regionally-specific blocks that were flash-frozen in N_2 and stored at −80°C.

Immunofluorescence

Specimens were fixed in paraformaldehyde, paraffin-embedded, and cut into 6-μm sections. Deparaffinized tissue sections were incubated in 3% H_2O_2, 97% methanol for 30 minutes at room temperature (RT), then washed 3 times with phosphate-buffered saline (PBS). The pretreatments prior to antibody labeling were as follows. For ApoE staining, the tissue sections were digested with the Digest-All 2 trypsin solution (Zymed/Invitrogen, Carlsbad, CA) for 10 minutes at 37°C. For βAPP staining, the sections were boiled in 1 mM EDTA (pH 8.0) for 10 minutes at medium power in a microwave. After 3 rinses in PBS, all sections were blocked (80% Dulbecco's Modified Eagle's Medium, 19% fetal calf serum, 1% bovine serum albumin) for one hour at RT. Following PBS rinses, sections were incubated in primary antibody solutions overnight at RT. Goat anti-human ApoE antibody (Calbiochem, La Jolla, CA) was used at 1:2,000, and mouse anti-βAPP antibody (Vector; Burlingame CA) was used at 1:100. Following PBS rinses, the secondary antibody was added. A rabbit anti-goat IgG conjugated to peroxidase (KPL, Gaithersburg, MD) was used at 1:200 dilution to detect the ApoE primary antibody, and a “prediluted” horse anti-mouse IgG conjugated to peroxidase (Vector) was further diluted 1:5 to detect the βAPP primary antibody. Development was achieved with tyramide signal amplification with Alexa Fluor 488 and 594 tyramide (Molecular Probes, Eugene, OR) using the manufacturer's recommended conditions. Prior to the addition of the second primary antibody in double-labeling experiments, slides were rinsed in PBS, incubated in 0.01 N HCl for 10 minutes at RT to inactivate peroxidase, rinsed again in PBS, and subjected to antigen-specific pretreatments, if necessary. Tissue sections were counterstained with 100 ng/ml 4′,6 diamino-2-phenylindole dihydrochloride (DAPI) for 5 minutes at RT in order to visualize cellular nuclei. The tissue sections were mounted with Vectashield antifade mounting medium (Vector) and stored at 4°C.

Image Analysis

Immunostained tissues were examined using a Nikon Eclipse E600 microscope with a Y-FL epifluorescence attachment. Images were captured at 20× magnification using a CoolSNAP ES digital camera (Roper Scientific, Ottobrunn, Germany) using identical conditions (exposure, gamma). Images were captured from the amygdala, hippocampus, and the parahippocampal gyrus. Thresholding and total fluorescence intensity calculations were done using the MetaVue 6.2r2 software package (Molecular Devices, Sunnyvale, CA). For quantitation of total ApoE fluorescence, a minimum threshold range (600–1000) was set for the grayscale images. Plaque-associated ApoE in each image was then determined by integrating the fluorescence intensity within plaques manually selected by integrated morphometry. The remainder was considered to be cytoplasmic ApoE. For quantitation of total βAPP, a minimum threshold range (300–600) was set for the grayscale images. For quantitation of somal βAPP, regions of interest were selected that comprised neuronal somata (cells with a nuclear diameter greater than 8 μm), and fluorescence intensity was determined by integrating pixels values within these structures. The remainder was considered to be neuritic βAPP. Demographic data, percent APOε4-positive alleles and Braak and Braak scores of the subjects used for this analysis are summarized in Table 2.

Neuronal Cultures

Cultures highly enriched for neocortical neurons were established from E18 rats or E17 mice, as described previously (29). Experiments using primary neuronal cell cultures were performed after 7 to 10 days in culture. The NTera2 human neuronal cell line (American

Type Culture Collection, Manassas, VA) was maintained in Dulbecco's modified Eagle medium (DMEM; Invitrogen/Life Technologies, Grand Island, NY) supplemented to 10% with fetal bovine serum (FBS). In some cases, cultures were treated with recombinant ApoE3 or ApoE4 (Invitrogen, Carlsbad CA) or receptor-associated protein, RAP (Calbiochem).

RNA Interference

The expression of ApoE was attenuated by the application of short, interfering RNA (siRNA), comprising synthetic double-stranded RNA, one strand of which corresponded to a 22-bp sequence in the mRNA of ApoE: 5′- GAC CAU GAA GGA GUU GAA Gtt. As a control, parallel cultures were exposed to synthetic double-stranded RNA of a sequence bearing no homology to known genes ("cRNA"). Dried RNA oligonucleotides were resuspended to 20 μM in nuclease-free water and stored at −70°C. Administration of siRNA or cRNA to cells utilized siPORT™ Lipid Transfection Agent (Ambion, Austin, TX) according to the manufacturer's instructions. For NTera2, 1.2×10^5 cells were seeded in a 6-well dish one day prior to transfection in 2 ml DMEM. A 100-μl aliquot of DMEM containing 5% FBS was mixed with 5 μl transfection reagent, and this mixture was incubated for 10 minutes at RT. This suspension was then combined with a separate 100-μl aliquot of DMEM/FBS containing 750 nM RNA, and this mixture was incubated for another 20 minutes at RT before application to cell cultures by addition to the existing culture medium. After optimization by monitoring ApoE levels, additional treatments were routinely applied 48 hours after application of the RNA/lipid complexes. Treatment of primary cortical neurons was performed similarly except that the cells were established in culture for 6 days prior to application of the RNA/lipid complexes.

Reverse Transcriptase-Polymerase Chain Reaction (RT-PCR)

Total RNA was extracted from cultured cells using TriReagent (Molecular Research Center, Inc., Cincinnati, OH) according to the manufacturer's instructions. For extraction from tissue, frozen specimens were pulverized with a mortar and pestle, and RNA was prepared from a portion of the pulverized material with the ToTALLY RNA kit (Ambion). Gel-based RT-PCR was performed as described previously (30). Levels of ApoE mRNA were normalized relative to those of glyceraldehyde-phosphate dehydrogenase (GAPDH) in the same sample. The sequences of primers for human ApoE were 5′-TTG AAG GCC TAC AAA TCG GAA CT (upstream) and 5′-CTG CTC CTT CAC CTC GTC CA (downstream). GAPDH primer sequences for human were 5′-AGG TCG GAG TCA ACG GAT TTG (upstream) and 5′-TGG CAG GTT TTT CTA GAC GGC (downstream). RT and PCR were performed using reagents from Clontech (Mountain View, CA). PCR amplification utilized 4 μl of RT product and was performed through 32 cycles for human ApoE at 94°C, 57°C, and 72°C (45 seconds each). For GAPDH, amplification was performed through 26 cycles at 94°C, 60°C, and 72°C (45 seconds each). The PCR reaction was stopped by final extension for 10 minutes at 72°C. Equal volumes of reaction mixture from each sample were loaded onto 1.2% agarose gels, and fluorescent images were digitally captured for analysis of intensity with NIH Image 1.60.

Real-time RT-PCR was performed on RNA assessed qualitatively and quantitatively on an Agilent Bioanalyzer (Agilent, Palo Alto, CA). The RT reaction utilized 500 ng RNA and TaqMan Reverse Transcription Reagents (including random hexamers for priming). PCR was performed with the Power SYBR-Green PCR Master Mix (Applied Biosystems, Foster City, CA) in an ABI 7900HT Fast Real-time PCR System (Applied Biosystems). The βAPP primers used were as follows: 5′-AAC CAC CGT GGA GCT CCT T (forward); 5′-ATG CCA CGG CTG GAG ATC (reverse). Equal amounts of RT-PCR from each sample were pooled to use for standard curve reactions with each primer set to verify linearity and a

suitable slope. A melting curve was generated for both βAPP and 18S rRNA to ensure that a single peak of the predicted T_m was produced and no primer-dimer complexes were present. RT-PCR signal was indexed to the efficiency of the RT reaction for each sample (31).

Western Immunoblot Assay

Proteins were extracted using lysis buffer (50 mM Tris-HCl, pH 7.5, 150 mM NaCl, 1% Nonidet P40, 0.5% sodium deoxycholate, and 0.1% SDS) and quantified using a Micro BCAassay reagent kit (Pierce, Rockford, IL) as described previously (32). Aliquots (30 μg for βAPP, 100 μg for ApoE) were loaded onto a 4% to 12% gradient Criterion XT Bis-Tris gel (BioRad Life Science, Hercules, CA), subjected to electrophoresis at 100V for 2.5 hours and transferred to nitrocellulose membranes. Blots were incubated for 2 hours with blocking buffer: 0.2% I-Block (Applied Biosystems) and 0.1% Tween-20 in PBS. They were then incubated 2 hours with goat anti-human ApoE (Calbiochem) or rabbit anti-β-Amyloid Protein Precursor (StressGen Biotechnologies, Corp., Ann Arbor, MI). After washing twice in PBS containing 0.1% Tween-20 (PBS-T), ApoE blots were incubated 1 hour with rabbit anti-goat IgG (Rockland Immunochemicals, Gilbertsville, PA); these blots or βAPP blots were then washed twice in PBS-T and incubated 1 hour with anti-rabbit secondary antibodies conjugated to alkaline phosphatase **(**Applied Biosystems). After additional washes, antibody binding was visualized using Western–Light™ Chemiluminescent Detection System (Applied Biosystems). Exposures were digitized and analyzed using NIH Image 1.60.

Statistical Analysis

Pairwise comparisons were made by Student *t*-test. Multifactorial data sets were analyzed by ANOVA and Scheffe *post-hoc* tests.

Results

Relationships between βAPP, ApoE, Aging, and Plaque-Related AD Pathology

βAPP—Tissue sections through the hippocampus of 8 non-demented individuals aged 29 to 81 years were analyzed for βAPP expression. A progressive increase in neuronal βAPP expression was observed with increasing age (Fig. 1). Although the increases detected in neuronal βAPP immunofluorescence may not correlate directly with absolute levels of protein, the data show a clear trend in βAPP increase in human brains from young to older adults

We expected that the development of AD pathology would entail an exaggeration of the stress of age-related changes and alterations in neuronal βAPP expression. For our preliminary analysis we surveyed regions of amygdala differentially affected by AD pathology, including the incipient deposition of Aβ in non-demented elderly individuals. Areas devoid of diffuse Aβ plaques (i.e. no pathology) were rare in the AD patients, but some such regions were found; conversely, areas with several neuritic Aβ plaques were rare but nonetheless present in some control patients. Surprisingly, immunodetectable levels of βAPP were lower in neurons in areas of the amygdala that contained a few Aβ plaques compared to those in regions (or specimens) that lacked plaques (Figs. 2, 3A). Levels of βAPP in plaque-rich regions were still lower than those in areas of the amygdala with a few plaques. Similar findings were observed in hippocampus (Figs. 2, 3B). Even within regions containing plaques, immunodetection of βAPP generally appeared higher in neurons distant from Aβ plaques than in those adjacent to diffuse plaques, and neuronal somata near mature plaques had lower levels of βAPP immunofluorescence than those observed in neurons near diffuse plaques (data not shown). These inverse relationships between βAPP expression and the degree of plaque pathology were independent of the pre-mortem diagnosis of dementia

(i.e. non-demented vs. AD). As we and others have reported, the abundance of βAPP in dystrophic neurites was confirmed in this broader view of spatial distribution (Fig. 2). Together, these data indicate that levels of βAPP in neuronal somata initially rise with pathology and aging (the latter presumably representing a trend towards incipient Aβ pathology), but then decline as AD-related pathology worsens. The βAPP that is present in AD appears to accumulate in dystrophic neurites.

Proteolytic processing of βAPP might contribute to a diminished somal immunofluorescence under conditions of AD pathogenesis. Therefore, we measured mRNA levels to distinguish between changes in stability and changes in expression of the βAPP gene. Real-time RT-PCR analyses indicated that the severity of AD pathology correlated with a decline of total βAPP mRNA levels (Fig. 4).

ApoE—As for βAPP, the levels of ApoE immunofluorescence in the hippocampus rose significantly across adult aging in non-demented adults (Fig. 1). ApoE expression was also elevated in regions affected in AD (Figs. 2, 3). In contrast to the profile seen for βAPP expression, however, ApoE levels continued to rise along with increasing severity of AD plaque pathology. This correlation was generally true for cell-associated ApoE. Because extracellular ApoE appeared to be relevant to the coordinate regulation of βAPP in our cell culture experiments (below), we also performed analyses that included extracellular ApoE immunofluorescence. These analyses showed very pronounced elevations of total ApoE immunofluorescence in specimens with abundant plaque pathology in both amygdala and hippocampus (Fig. 3, “Total ApoE”).

Glutamate-Induced Expression of βAPP Is ApoE-Dependent

Several forms of stress or injury are capable of elevating neuronal expressions of both βAPP and ApoE. We have been particularly interested in excitotoxic stress induced by glutamate released from microglia under inflammatory conditions (33,34). Therefore, we assayed levels of βAPP and ApoE mRNA and protein in neuronal cultures treated with marginally toxic concentrations of glutamate. Primary cultures of rodent cortical neurons responded to 20 μM glutamate with elevations of both ApoE and βAPP (Fig. 5). Because ApoE is a secreted protein capable of both autocrine and paracrine effects, we tested its contribution to the induction of βAPP by glutamate. Treatment of NTera2 cells with siRNA directed against ApoE successfully reduced levels of the protein, including its elevation by glutamate treatment whereas the control scrambled sequence of double-stranded RNA had no impact on ApoE levels (Fig. 6A). Interestingly, cultures in which ApoE levels were suppressed did not show an elevation of βAPP (Figs. 6B, 7B, C). Similar results were obtained with primary cortical neurons (Fig. 7A).

The requirement for ApoE in glutamate-induced increases in βAPP could involve intracellular or extracellular roles for ApoE. To test the mode of action, we applied receptor-associated protein (RAP) to interfere with ApoE binding to receptors of the LRP class. Similar to the effect of ApoE siRNA, RAP blocked glutamate-evoked elevations of βAPP levels (Fig. 8). These results suggest that the induction of βAPP levels in response to glutamate might be entirely secondary to an elevation of ApoE. We tested the sufficiency of ApoE in this regard by adding recombinant protein directly to primary neuron cultures. ApoE3 induced βAPP expression under these conditions whereas ApoE4 did not (Fig. 9).

Discussion

We previously reported a high degree of βAPP immunoreactivity in dystrophic neurites that lie in and near the most obvious sites of Aβ deposition (35). This raises the overlooked question of distribution, i.e. whether neuronal βAPP is generally elevated in AD or whether

the rise is spatially restricted to plaque regions. We report here that the only apparent elevation of βAPP in AD—indeed, the only notable expression of βAPP—is restricted to dystrophic neurites in and around amyloid plaques. While ApoE continued to rise with the progression of amyloid pathology, βAPP underwent a dramatic decline in expression in neuronal somata. A corresponding decline in βAPP mRNA suggests a drop in gene expression rather than accelerated removal of protein via processing. Thus, this plaque-dependent reversal of the age-related rise in neuronal βAPP is analogous to the attenuation of βAPP induction we observed when ApoE expression or activity was blocked in neuronal cell cultures. Given the important roles of βAPP in neuromodulation and neuroprotection, we suggest that reduction of βAPP expression over the course of AD may contribute to the vulnerability of cortical neurons.

Kimura et al reported an age-related redistribution of βAPP immunoreactivity from neuronal somata to dystrophic neurites in neuritic Aβ plaques in the brains of cynomolgus monkeys (36). The trends observed here were apparent both as a function of the extent of Aβ deposition and as a function of spatial proximity to mature plaques. ApoE staining was most abundant in plaques, and βAPP staining was most abundant in the dystrophic neurites in and around mature plaques. An elevation of βAPP, as we have shown for conditions of cellular stress and neuroinflammation, has been speculated to contribute directly to AD pathogenesis. As the source of Aβ, βAPP may contribute a simple mass-action tipping point when chronically elevated. Indeed, the recent discovery of families bearing duplication of the *App* gene (which results in 3 copies of the gene) makes the pathological implications of a persistent excess of βAPP clear (6,7).

Regardless of the potential contributions of βAPP to amyloidogenesis, it is also evident that βAPP is part of an acute-phase response to injury that provides neuroprotection. Neurons from βAPP-knockout mice show reduced viability (37), and such mice present with deficits in long-term potentiation and memory-related behavior (2). Overexpression of βAPP through transgenesis also protects against the neurotoxicity of kainate and the HIV protein gp120 (3). Detrimental effects have been observed when the βAPP being overexpressed is a poor substrate for α-secretase (38). This is consistent with the neuroprotective activity demonstrated for the secreted product sAPPα in models of ischemic (39) and traumatic (40) injury. The distinction between beneficial and pathogenic contributions by βAPP probably involves nuances of its processing into various proteolytic fragments; these distinctions may rest, in part, with subtleties of βAPP localization.

The age-related elevation of somal ®APP may indicate a response to the earliest stages of A® accumulation. A trend in this direction was noted in low-plaque regions of hippocampus (Fig. 3B). Amyloid deposition increases with age (41); soluble or otherwise surreptitious A® is likely to be on the rise as a common consequence of aging, as well (42). It is possible that the initial impact of an A® elevation includes inductions of ApoE and βAPP expression, such that these 2 proteins are simultaneously elevated upon the initial accumulation of A® temporally but also upon the initial encounter of individual cells with the edge of an A® gradient that emanates from a plaque in established disease.

Based on our present data, glutamate could be a primary stimulus for ApoE induction during AD pathogenesis. Microglia release large amounts of glutamate when they are activated by secreted forms of βAPP or by Aβ (34,43,44). Although some reports indicate a depletion of whole-tissue glutamate concentration in end-stage AD, glutamatergic axonal boutons undergo a transient increase during the intermediate stages of AD pathology (45–47). The ability of ApoE to protect against microglia-produced glutamate (48) strengthens the inference that ApoE is elevated as a compensatory change.

Neuronal expression of ApoE has been controversial. Rodent studies typically show very low or undetectable levels of ApoE in CNS neurons whereas human neurons appear to have a moderate level of expression, probably due to species differences in the ApoE promoter sequence (49). Even in rodent neurons, however, ApoE expression may be induced under extraordinary circumstances. The activity of the ApoE promoter is reportedly regulated by the Sp1 family of transcription factors (50). We have documented a replacement of the transactivating Sp1 by Sp4 in cortical neurons (51), and this results in a transcriptional repression with respect to at least one promoter element (52). We have also found that Sp4 is degraded by the calcium-dependent protease calpain in glutamate-treated neurons (51), perhaps relieving some genes of the suppressive influence of Sp4. We therefore speculate that elevation of ApoE expression in neurons involves the degradation of a neuron-specific transcriptional repressor.

To assess the role of ApoE role in βAPP induction, we applied recombinant ApoE to primary cortical neurons. Although this form of the protein is rather unrelated to the structural complexity found in lipoprotein particles, it is clear now that the ApoE that prevails in interstitial fluid in the CNS is also quite different from the lipoprotein complexes present in plasma. Indeed, it probably even differs from the ApoE found in CSF. Apolipoprotein/lipid complexes are formed during translation of the protein by a process dependent upon cell type-specific machinery (53,54). Astrocytes appear incapable of generating the same lipoprotein complexes found in plasma or even cerebrospinal fluid (55,56). It is likely that the ApoE induced in neurons is at least as structurally simplistic as that expressed by astrocytes.

It is intriguing that ApoE3 was capable of inducing βAPP whereas ApoE4 was not. Possession of the ε4 allele of ApoE imparts a dose-dependent elevation in AD risk (12). The specificity of the effects we observed suggests that recombinant ApoE may possess at least some aspect of a structural determinant relevant to AD pathogenesis. Persons in whom ApoE4 comprises a sizable fraction of the total brain ApoE might lack the ability to induce βAPP as robustly and this hypothesis would predict that they lose neuronal βAPP expression earlier.

Once plaque pathology becomes apparent, we found that βAPP levels in neuronal somata begin to drop. This effect was even detectable near diffuse plaques. Although these deposits are often considered to be of little neuropathological consequence, we have previously documented their impact on astrocytes (57), microglia (35), and neurons (58) in the vicinity of diffuse plaques. It is tempting to speculate that the βAPP decline reflects some interference with the glutamate→ ApoE→βAPP axis demonstrated in vitro. Indeed, the disease process might proceed in a manner analogous to our experimental manipulations of ApoE levels or activity by siRNA and RAP. Because ApoE levels correlated with severity of AD pathology, it seems most likely that any interference in the axis would come downstream of ApoE production. Given the dramatic increases in extracellular ApoE in AD (e.g. as deduced by subtraction of the cellular levels from the totals in Fig. 3), and the spatial restriction of these extracellular pools to the amyloid plaques, we hypothesize that interruption of the glutamate→ApoE→ βAPP axis would result from sequestration of the ApoE into plaques. This concept is supported by our finding that βAPP first declines near diffuse plaques because diffuse, newly formed plaques already show significant ApoE accumulation (59). We are currently using *in vitro* approaches to test the capacity of Aβ to deplete ApoE activity. Most cell culture studies have indicated that Aβ potentiates the excitotoxicity of glutamate (60–62). An emerging body of data, however, suggests that Aβ inhibits post-synaptic responses to glutamate (63–65). Predictions about the interaction of Aβ with the glutamate→ApoE→βAPP axis are further complicated by the fact that ApoE binds Aβ, inhibiting its neurotoxicity (66).

The observed decline of immunoreactive somal βAPP corresponded to a decline in βAPP mRNA through the progression of disease, consistent with *in situ* hybridization findings reported by Tanzi *et al* (67). These data suggest that βAPP expression is interrupted at the transcriptional level. Our in vitro observations in which ApoE depletion correlated with a drop in βAPP mRNA levels), therefore, also correlate with in situ findings. The rise of βAPP immunofluorescence in dystrophic neurites may thus represent accumulation of protein that is independent of *de novo* synthesis, i.e. decreased degradation. This might involve interruption of normal axonal transport, presumably due to abnormalities in microtubule integrity and/or molecular motors such as dynein and kinesin (68).

Acknowledgments

The authors appreciate the technical contributions of Richard Jones and Marjorie Beggs.

These studies were supported by NIA (P01AG12411).

References

1. Rosen DR, Martin-Morris L, Luo LQ, et al. A Drosophila gene encoding a protein resembling the human β-amyloid protein precursor. Proc Natl Acad Sci U S A. 1989; 86:2478–82. [PubMed: 2494667]
2. Dawson GR, Seabrook GR, Zheng H, et al. Age-related cognitive deficits, impaired long-term potentiation and reduction in synaptic marker density in mice lacking the beta-amyloid precursor protein. Neuroscience. 1999; 90:1–13. [PubMed: 10188929]
3. Masliah E, Westland CE, Rockenstein EM, et al. Amyloid precursor proteins protect neurons of transgenic mice against acute and chronic excitotoxic injuries in vivo. Neuroscience. 1997; 78:135–46. [PubMed: 9135095]
4. Prasher VP, Farrer MJ, Kessling AM, et al. Molecular mapping of Alzheimer-type dementia in Down's syndrome. Ann Neurol. 1998; 43:380–83. [PubMed: 9506555]
5. Griffin WS, Sheng JG, McKenzie JE, et al. Life-long overexpression of S100beta in Down's syndrome: implications for Alzheimer pathogenesis. Neurobiol Aging. 1998; 19:401–405. [PubMed: 9880042]
6. Rovelet-Lecrux A, Hannequin D, Raux G, et al. APP locus duplication causes autosomal dominant early-onset Alzheimer disease with cerebral amyloid angiopathy. Nat Genet. 2006; 38:24–26. [PubMed: 16369530]
7. Sleegers K, Brouwers N, Gijselinck I, et al. APP duplication is sufficient to cause early onset Alzheimer's dementia with cerebral amyloid angiopathy. Brain. 2006; 129:2977–83. [PubMed: 16921174]
8. Moir RD, Lynch T, Bush AI, et al. Relative increase in Alzheimer's disease of soluble forms of cerebral Abeta amyloid protein precursor containing the Kunitz protease inhibitory domain. J Biol Chem. 1998; 273:5013–19. [PubMed: 9478949]
9. Panegyres PK, Zafiris-Toufexis K, Kakulas BA. Amyloid precursor protein gene isoforms in Alzheimer disease and other neurodegenerative disorders. J Neurol Sci. 2000; 173:81–92. [PubMed: 10675649]
10. Harrison PJ, Barton AJ, Procter AW, et al. The effects of Alzheimer's disease, other dementias, and premortem course on beta-amyloid precursor protein messenger RNA in frontal cortex. J Neurochem. 1994; 62:635–44. [PubMed: 8294927]
11. Choi BH, Kim RC, Vaughan PJ, et al. Decreases in protease nexins in Alzheimer's disease brain. Neurobiol Aging. 1995; 16:557–62. [PubMed: 8544905]
12. Corder EH, Saunders AM, Strittmatter WJ, et al. Gene dose of apolipoprotein E type 4 allele and the risk of Alzheimer's disease in late onset families. Science. 1993; 261:921–23. [PubMed: 8346443]

13. Namba Y, Tomonaga M, Kawasaki H, et al. Apolipoprotein E immunoreactivity in cerebral amyloid deposits and neurofibrillary tangles in Alzheimer's disease and kuru plaque amyloid in Creutzfeldt-Jakob disease. Brain Res. 1991; 541:163–66. [PubMed: 2029618]
14. Nicoll JR, Roberts GW, Graham DI. Apolipoprotein E ε4 allele is associated with deposition of amyloid β-protein following head injury. Nat Med. 1995; 1:135–37. [PubMed: 7585009]
15. Sheng JG, Mrak RE, Griffin WS. Apolipoprotein E distribution among different plaque types in Alzheimer's disease: Implications for its role in plaque progression. Neuropathol Appl Neurobiol. 1996; 22:334–41. [PubMed: 8875468]
16. Bales KR, Verina T, Cummins DJ, et al. Apolipoprotein E is essential for amyloid deposition in the APP(V717F) transgenic mouse model of Alzheimer's disease. Proc Natl Acad Sci U S A. 1999; 96:15233–38. [PubMed: 10611368]
17. Wisniewski T, Castano EM, Golabek A, et al. Acceleration of Alzheimer's fibril formation by apolipoprotein E in vitro. Am J Pathol. 1994; 145:1030–35. [PubMed: 7977635]
18. Nathan BP, Bellosta S, Sanan DA, et al. Differential effects of apolipoproteins E3 and E4 on neuronal growth in vitro. Science. 1994; 264:850–52. [PubMed: 8171342]
19. Strittmatter WJ, Saunders AM, Goedert M, et al. Isoform-specific interactions of apolipoprotein E with microtubule-associated protein tau: Implications for Alzheimer disease. Proc Natl Acad Sci USA. 1994; 91:11183–86. [PubMed: 7972031]
20. Tesseur I, Van Dorpe J, Spittaels K, et al. Expression of human apolipoprotein E4 in neurons causes hyperphosphorylation of protein tau in the brains of transgenic mice. Am J Pathol. 2000; 156:951–64. [PubMed: 10702411]
21. Huang Y, Liu XQ, Wyss-Coray T, et al. Apolipoprotein E fragments present in Alzheimer's disease brains induce neurofibrillary tangle-like intracellular inclusions in neurons. Proc Natl Acad Sci U S A. 2001; 98:8838–43. [PubMed: 11447277]
22. Harris FM, Brecht WJ, Xu Q, et al. Carboxyl-terminal-truncated apolipoprotein E4 causes Alzheimer's disease-like neurodegeneration and behavioral deficits in transgenic mice. Proc Natl Acad Sci U S A. 2003; 100:10966–71. [PubMed: 12939405]
23. White F, Nicoll JA, Horsburgh K. Alterations in ApoE and ApoJ in relation to degeneration and regeneration in a mouse model of entorhinal cortex lesion. Exp Neurol. 2001; 169:307–18. [PubMed: 11358444]
24. Kay AD, Petzold A, Kerr M, et al. Cerebrospinal fluid apolipoprotein E concentration decreases after traumatic brain injury. J Neurotrauma. 2003; 20:243–50. [PubMed: 12820678]
25. Wenham PR, Price WH, Blandell G. Apolipoprotein E genotyping by one-stage PCR. Lancet. 1991; 337:1158–59. [PubMed: 1674030]
26. Aging NIo, disease tRIWGoDCftNAoAs. Consensus recommendations for the postmortem diagnosis of Alzheimer's disease. The National Institute on Aging, and Reagan Institute Working Group on Diagnostic Criteria for the Neuropathological Assessment of Alzheimer's Disease. Neurobiol Aging. 1997; 18:S1–2. [PubMed: 9330978]
27. Mirra SS, Heyman A, McKeel D, et al. The Consortium to Establish a Registry for Alzheimer's Disease (CERAD). Part II. Standardization of the neuropathologic assessment of Alzheimer's disease. Neurology. 1991; 41:479–86. [PubMed: 2011243]
28. Braak H, Braak E. Neuropathological stageing of Alzheimer-related changes. Acta Neuropathologica. 1991; 82:239–59. [PubMed: 1759558]
29. Liu L, Li Y, Van Eldik LJ, et al. S100B-induced microglial and neuronal IL-1 expression is mediated by cell type-specific transcription factors. J Neurochem. 2005; 92:546–53. [PubMed: 15659225]
30. Li Y, Liu L, Barger SW, et al. Vitamin E suppression of microglial activation is neuroprotective. J Neurosci Res. 2001; 66:163–70. [PubMed: 11592111]
31. Libus J, Storchova H. Quantification of cDNA generated by reverse transcription of total RNA provides a simple alternative tool for quantitative RT-PCR normalization. Biotechniques. 2006; 41:156, 158, 160. passim. [PubMed: 16925017]
32. Li Y, Wang J, Sheng JG, et al. S100β increases levels of β-amyloid precursor protein and its encoding mRNA in rat neuronal cultures. J Neurochem. 1998; 71:1421–28. [PubMed: 9751173]

33. Barger SW. An unconventional hypothesis of oxidation in Alzheimer's disease: intersections with excitotoxicity. Front Biosci. 2004; 9:3286–95. [PubMed: 15353358]
34. Barger SW, Goodwin ME, Porter MM, et al. Glutamate release from activated microglia requires the oxidative burst and lipid peroxidation. J Neurochem. 2007; 101:1205–13. [PubMed: 17403030]
35. Griffin WS, Sheng JG, Roberts GW, et al. Interleukin-1 expression in different plaque types in Alzheimer's disease: significance in plaque evolution. J Neuropathol Exp Neurol. 1995; 54:276–81. [PubMed: 7876895]
36. Kimura N, Tanemura K, Nakamura S, et al. Age-related changes of Alzheimer's disease-associated proteins in cynomolgus monkey brains. Biochem Biophys Res Commun. 2003; 310:303–11. [PubMed: 14521910]
37. Perez RG, Zheng H, Van der Ploeg LH, et al. The β-amyloid precursor protein of Alzheimer's disease enhances neuron viability and modulates neuronal polarity. J Neurosci. 1997; 17:9407–14. [PubMed: 9390996]
38. Moechars D, Lorent K, De Strooper B, et al. Expression in brain of amyloid precursor protein mutated in the alpha-secretase site causes disturbed behavior, neuronal degeneration and premature death in transgenic mice. Embo J. 1996; 15:1265–74. [PubMed: 8635459]
39. Smith-Swintosky VL, Pettigrew LC, Craddock SD, et al. Secreted forms of amyloid precursor protein protect against transient cerebral ischemia in rats. J Neurochem. 1994; 63:781–84. [PubMed: 8035204]
40. Thornton E, Vink R, Blumbergs PC, et al. Soluble amyloid precursor protein alpha reduces neuronal injury and improves functional outcome following diffuse traumatic brain injury in rats. Brain Res. 2006; 1094:38–46. [PubMed: 16697978]
41. Braak H, Braak E. Frequency of stages of Alzheimer-related lesions in different age categories. Neurobiol Aging. 1997; 18:351–57. [PubMed: 9330961]
42. Lindner MD, Hogan JB, Krause RG, et al. Soluble Abeta and cognitive function in aged F-344 rats and Tg2576 mice. Behav Brain Res. 2006; 173:62–75. [PubMed: 16828889]
43. Barger SW, Basile AS. Activation of microglia by secreted amyloid precursor protein evokes release of glutamate by cystine exchange and attenuates synaptic function. J Neurochem. 2001; 76:846–54. [PubMed: 11158256]
44. Ikezu T, Luo X, Weber GA, et al. Amyloid precursor protein-processing products affect mononuclear phagocyte activation: Pathways for sAPP- and Abeta-mediated neurotoxicity. J Neurochem. 2003; 85:925–34. [PubMed: 12716424]
45. Bell KF, de Kort GJ, Steggerda S, et al. Structural involvement of the glutamatergic presynaptic boutons in a transgenic mouse model expressing early onset amyloid pathology. Neurosci Lett. 2003; 353:143–47. [PubMed: 14664921]
46. Bell KF, Bennett DA, Cuello AC. Paradoxical upregulation of glutamatergic presynaptic boutons during mild cognitive impairment. J Neurosci. 2007; 27:10810–17. [PubMed: 17913914]
47. Bell KF, Ducatenzeiler A, Ribeiro-da-Silva A, et al. The amyloid pathology progresses in a neurotransmitter-specific manner. Neurobiol Aging. 2006; 27:1644–57. [PubMed: 16271419]
48. Qin S, Colin C, Hinners I, et al. System Xc- and apolipoprotein E expressed by microglia have opposite effects on the neurotoxicity of amyloid-beta peptide 1-40. J Neurosci. 2006; 26:3345–56. [PubMed: 16554485]
49. Roses AD, Gilbert J, Xu PT, et al. Cis-acting human ApoE tissue expression element is associated with human pattern of intraneuronal ApoE in transgenic mice. Neurobiol Aging. 1998; 19:S53–58. [PubMed: 9562469]
50. Chang DJ, Paik YK, Leren TP, et al. Characterization of a human apolipoprotein E gene enhancer element and its associated protein factors. J Biol Chem. 1990; 265:9496–9504. [PubMed: 2188976]
51. Mao X, Yang SH, Simpkins JW, et al. Glutamate receptor activation evokes calpain-mediated degradation of Sp3 and Sp4, the prominent Sp-family transcription factors in neurons. J Neurochem. 2007; 100:1300–14. [PubMed: 17316402]

52. Mao X, Moerman-Herzog AM, Wang W, et al. Differential transcriptional control of the superoxide dismutase-2 κB element in neurons and astrocytes. J Biol Chem. 2006; 281:35863–72. [PubMed: 17023425]
53. Fazio S, Yao Z. The enhanced association of apolipoprotein E with apolipoprotein B-containing lipoproteins in serum-stimulated hepatocytes occurs intracellularly. Arterioscler Thromb Vasc Biol. 1995; 15:593–600. [PubMed: 7749873]
54. Wang S, McLeod RS, Gordon DA, et al. The microsomal triglyceride transfer protein facilitates assembly and secretion of apolipoprotein B-containing lipoproteins and decreases cotranslational degradation of apolipoprotein B in transfected COS-7 cells. J Biol Chem. 1996; 271:14124–33. [PubMed: 8662886]
55. LaDu MJ, Gilligan SM, Lukens JR, et al. Nascent astrocyte particles differ from lipoproteins in CSF. J Neurochem. 1998; 70:2070–81. [PubMed: 9572293]
56. Legleiter J, DeMattos RB, Holtzman DM, et al. In situ AFM studies of astrocyte-secreted apolipoprotein E- and J-containing lipoproteins. J Colloid Interface Sci. 2004; 278:96–106. [PubMed: 15313642]
57. Mrak RE, Sheng JG, Griffin WST. Correlation of astrocytic S100β expression with dystrophic neurites in amyloid plaques of Alzheimer's disease. J Neuropathol Exp Neurol. 1996; 55:273–79. [PubMed: 8786385]
58. Sheng JG, Zhou XQ, Mrak RE, et al. Progressive neuronal injury associated with amyloid plaque formation in Alzheimer disease. J Neuropathol Exp Neurol. 1998; 57:714–17. [PubMed: 9690675]
59. Thal DR, Capetillo-Zarate E, Schultz C, et al. Apolipoprotein E co-localizes with newly formed amyloid beta-protein (Abeta) deposits lacking immunoreactivity against N-terminal epitopes of Abeta in a genotype-dependent manner. Acta Neuropathol. 2005; 110:459–71. [PubMed: 16195918]
60. Koh JY, Yang LL, Cotman CW. β-amyloid protein increases the vulnerability of cultured cortical neurons to excitotoxic damage. Brain Res. 1990; 533:315–20. [PubMed: 2289145]
61. Mattson MP, Cheng B, Davis D, et al. Aβ peptides destabilize calcium homeostasis and render human cortical neurons vulnerable to excitotoxicity. J Neurosci. 1992; 12:379–89.
62. Gray CW, Patel AJ. Neurodegeneration mediated by glutamate and beta-amyloid peptide: a comparison and possible interaction. Brain Res. 1995; 691:169–79. [PubMed: 8590049]
63. Almeida CG, Tampellini D, Takahashi RH, et al. Beta-amyloid accumulation in APP mutant neurons reduces PSD-95 and GluR1 in synapses. Neurobiol Dis. 2005; 20:187–98. [PubMed: 16242627]
64. Hsieh H, Boehm J, Sato C, et al. AMPAR removal underlies Abeta-induced synaptic depression and dendritic spine loss. Neuron. 2006; 52:831–43. [PubMed: 17145504]
65. Shankar GM, Bloodgood BL, Townsend M, et al. Natural oligomers of the Alzheimer amyloid-beta protein induce reversible synapse loss by modulating an NMDA-type glutamate receptor-dependent signaling pathway. J Neurosci. 2007; 27:2866–75. [PubMed: 17360908]
66. Jordan J, Galindo MF, Miller RJ, et al. Isoform-specific effect of apolipoprotein E on cell survival and beta-amyloid-induced toxicity in rat hippocampal pyramidal neuronal cultures. J Neurosci. 1998; 18:195–204. [PubMed: 9412500]
67. Tanzi RE, Wenniger JJ, Hyman BT. Cellular specificity and regional distribution of amyloid beta protein precursor alternative transcripts are unaltered in Alzheimer hippocampal formation. Brain Res Mol Brain Res. 1993; 18:246–52. [PubMed: 8497186]
68. Stokin GB, Goldstein LS. Axonal transport and Alzheimer's disease. Annu Rev Biochem. 2006; 75:607–27. [PubMed: 16756504]

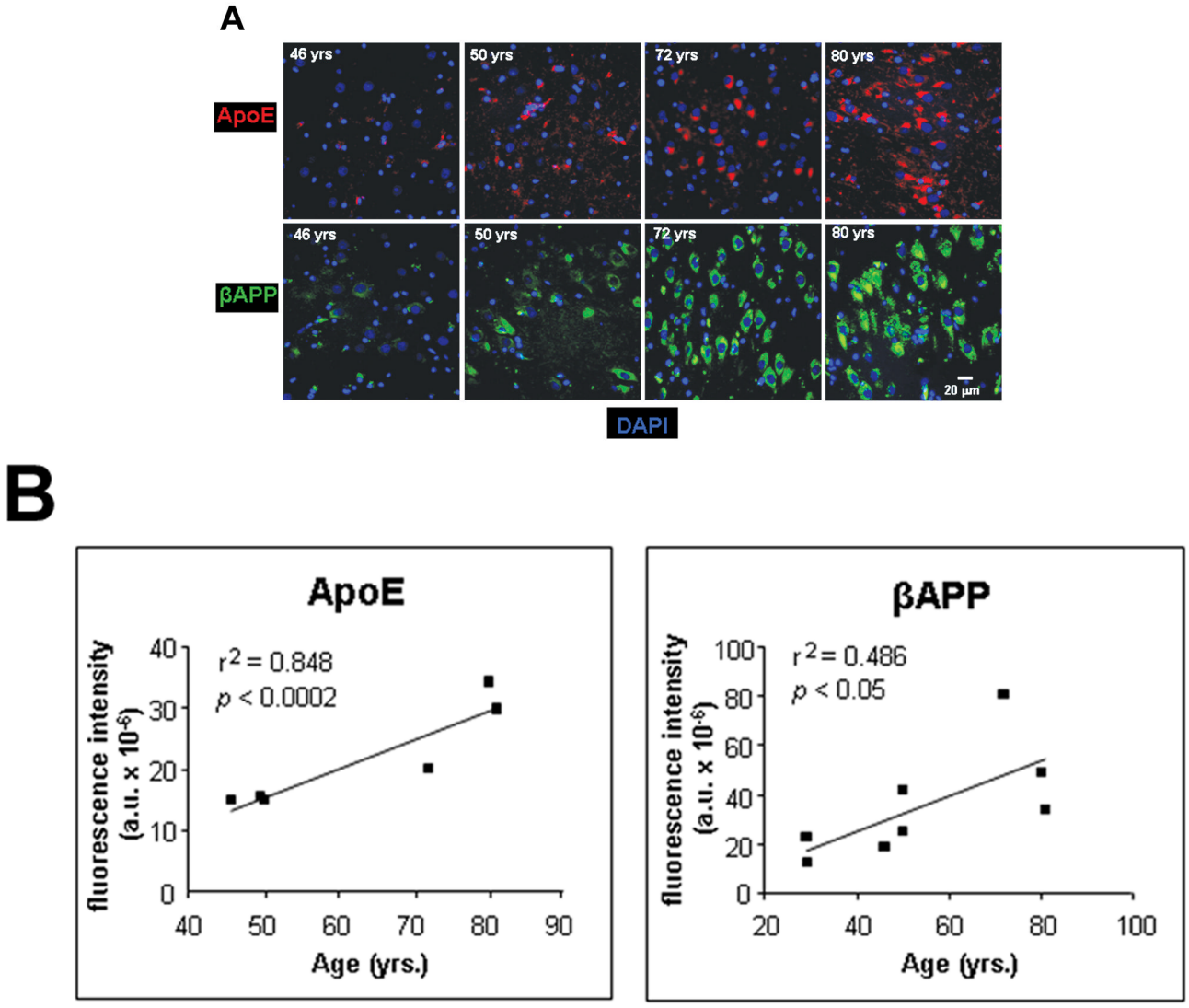

Figure 1.

Age-related changes in expression of βAPP and ApoE. **(A)** βAPP (green) and ApoE (red) were detected by immunofluorescence in tissue sections from hippocampus at the level of the lateral geniculate nucleus. Results are shown for 4 non-demented individuals across an age span of 46 to 80 years. Blue represents DAPI staining of cellular DNA. Images were digitized at 20× magnification. Scale bar represents 20 μm. **(B)** Quantitation of βAPP and ApoE immunofluorescence intensity was obtained by thresholding βAPP grayscale images and integrating pixels as described in Materials and Methods. Values reflect the mean of 3 images per hippocampus of 6 (ApoE) or 8 (βAPP) non-demented individuals.

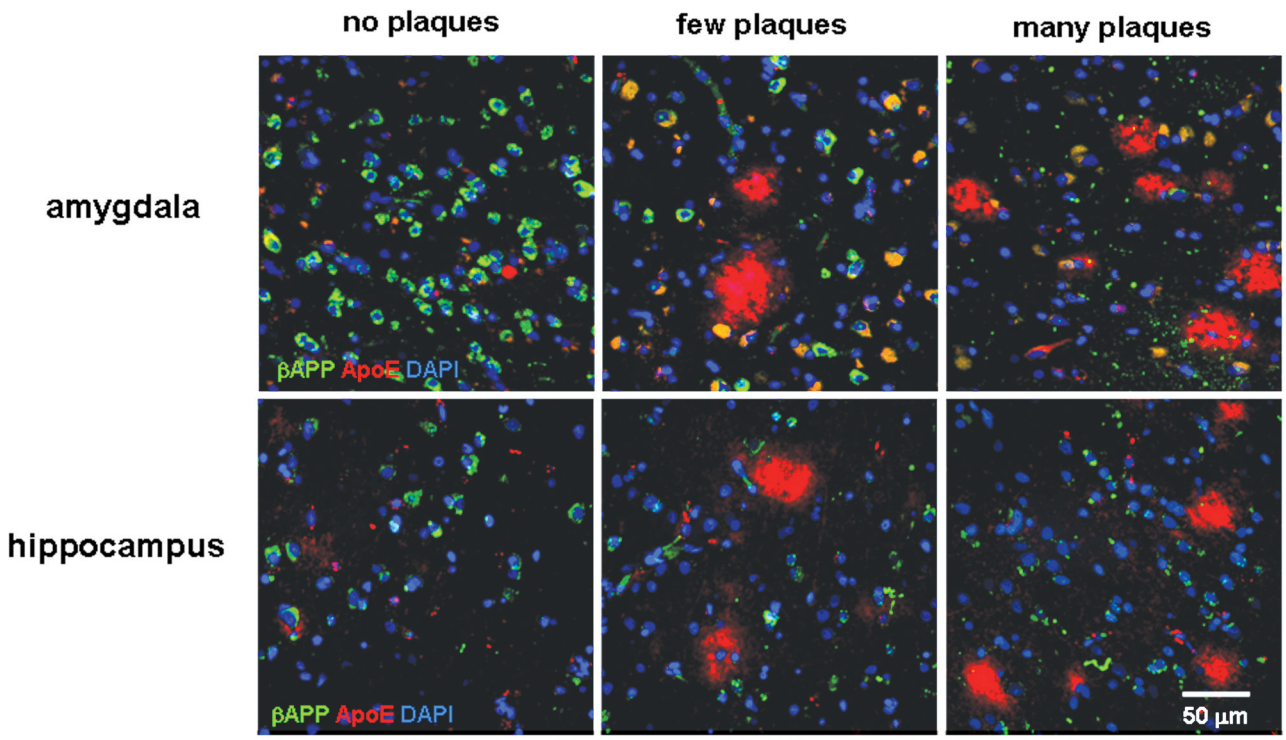

Figure 2.

βAPP levels decrease and ApoE levels increase with advancing AD pathology. βAPP (green) and ApoE (red) were detected in areas of amygdala or hippocampus with no Aβ deposits, a few Aβ plaques, or multiple Aβ plaques. Colocalization of βAPP and ApoE in neurons appears yellow-green. Blue is DAPI staining of cellular DNA. Note the increased βAPP-positive dystrophic neurites in the panels with many plaques. The scale bar represents 50 μm.

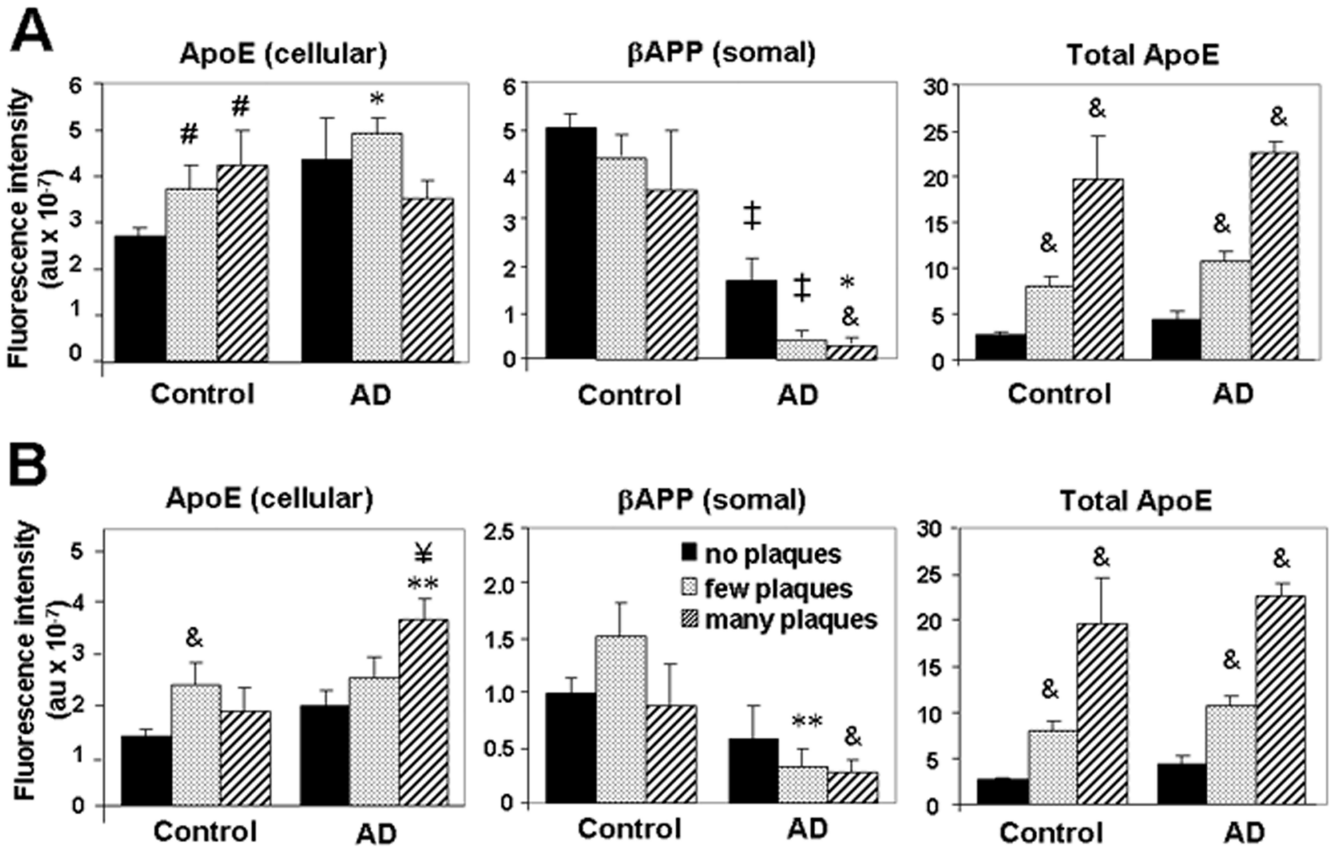

Figure 3.

βAPP and ApoE are differentially modulated in relation to plaque pathology. Intensities of βAPP fluorescence in neuronal somata, ApoE fluorescence in any cellular compartment, and total ApoE fluorescence were determined using analyses described in Materials and Methods. Fields were grouped according to "no plaques" (0), "few plaques" (1–4), or "many plaques" (≥5), in amygdala (**A**) or hippocampus (**B**). Values reflect the mean ± SEM from 13 (no plaques), 12 (few plaques), or 7 (many plaques) individuals. $^{\&}$ $p < 0.02$, $^{\#}$ $p < 0.05$ vs. control, no plaques; ‡ $p < 0.001$, ** $p < 0.01$, * $p < 0.05$ vs. corresponding control value; $^{¥}$ $p < 0.01$ vs. AD, no plaques.

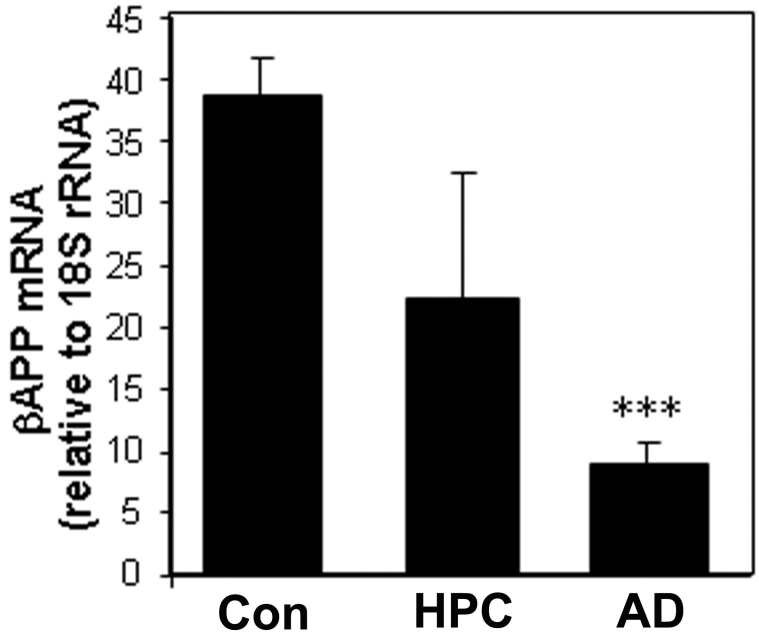

Figure 4.

βAPP mRNA declines in AD initiation and progression. Total RNA was extracted from amygdala of brains diagnosed as control, AD (n = 5), or high-pathology controls (HPC; clinically nondemented but with AD pathology; n = 3). RNA was subjected to qRT-PCR and scaled relative to input RNA quantity in a standard curve. Final values were corrected by the signal for 18S rRNA. ***$p < 0.00006$ vs. control (Student *t*-test)

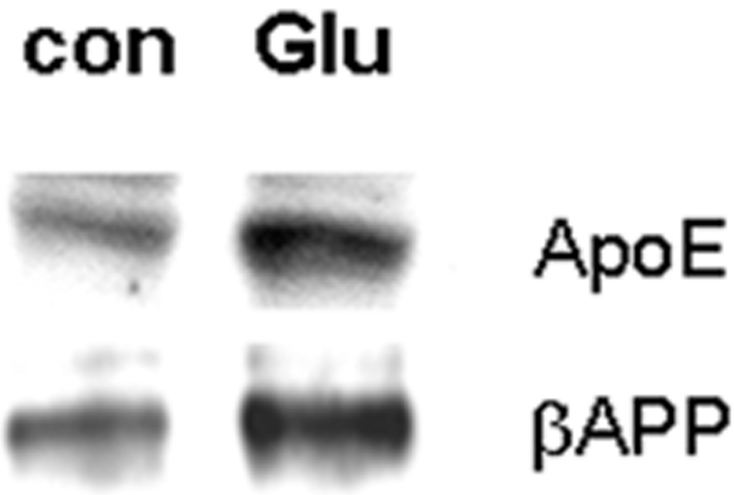

Figure 5.
Glutamate elevates ApoE and βAPP levels coordinately in primary neuronal cultures. Primary cortical neurons were left untreated or exposed to 20 μM glutamate for 20 hours, and then βAPP and ApoE were assessed by Western blot analysis. Data are representative of >10 experiments.

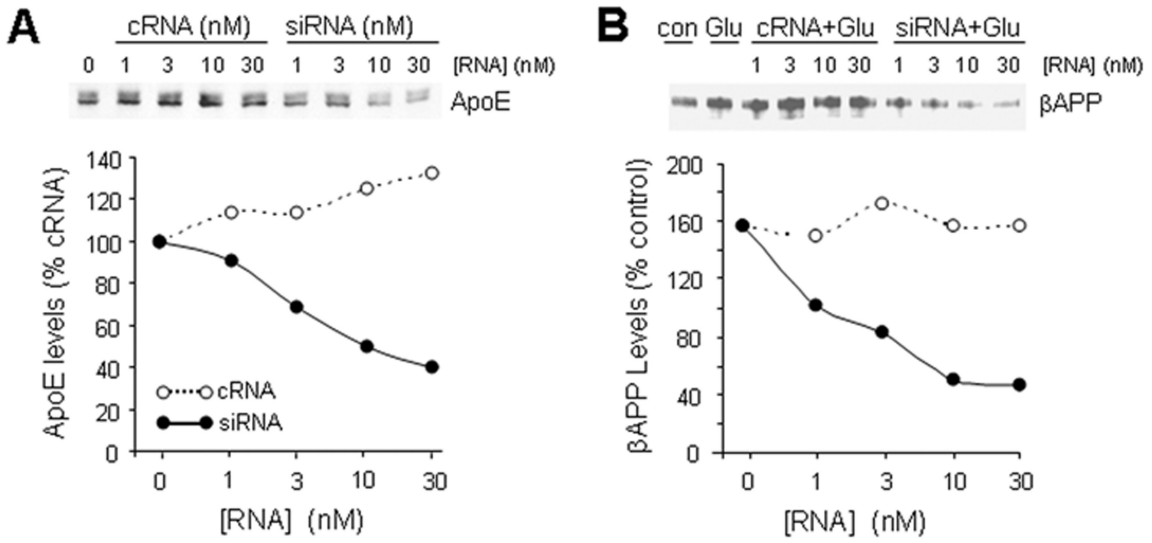

Figure 6.

Glutamate-induced elevation of βAPP is dependent upon ApoE expression. **(A)** The human neuronal cell line NTera2 was treated for 48 hours with the indicated concentrations of control RNA ("cRNA"; open circles) or siRNA directed against ApoE (filled circles). ApoE levels were assayed by Western blot analysis to verify effectiveness of siRNA. (**B)** NTera2 cells were treated with ApoE siRNA (filled circles), cRNA (open circles) or no RNA (lanes 1 and 2). After 48 hours, glutamate (20 μM) was applied to all but one set of cultures (lane 1). After 20 hours, βAPP levels were assayed by Western blot analysis. In both **A** and **B**, 1-way ANOVA indicates significant differences between the control and siRNA curves ($p < 0.008$).

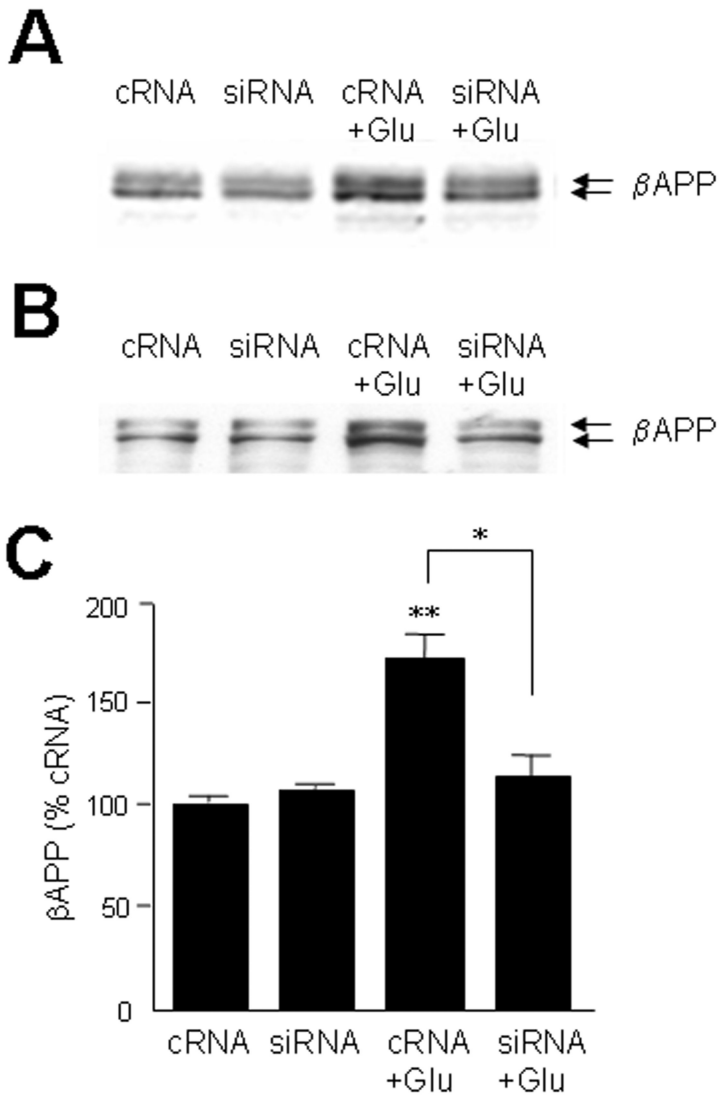

Figure 7.

Glutamate→ApoE→βAPP axis manifest in neuronal cultures. Cultures of primary rat cortical neurons (**A**) or NTera2 cells (**B**) were treated for 48 hours with 30 nM cRNA or siRNA directed against ApoE. Glutamate (20 μM) was then applied for 20 hours, after which βAPP levels were assayed by Western blot analysis. (**C)** Results from 3 experiments with NTera2 cells were quantified; *$p < 0.05$, siRNA+Glu vs. cRNA+Glu, **$p < 0.01$ cRNA+Glu vs. cRNA alone.

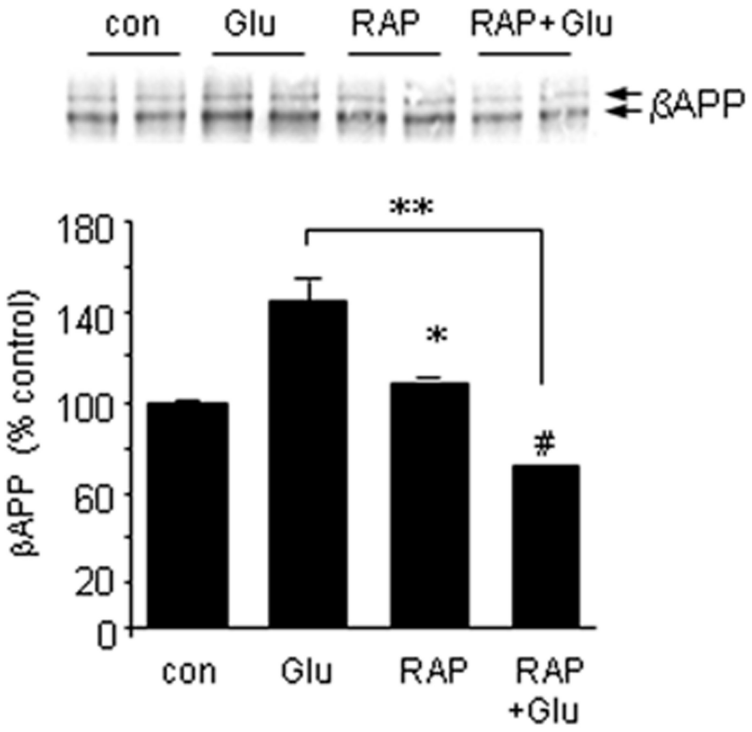

Figure 8.

LRP-ApoE interactions modulate glutamate induction of βAPP. NTera2 cells were treated with 20 μM glutamate in the presence or absence of 200 nM receptor-associated protein (RAP); additional cultures were treated with RAP alone. βAPP expression was determined 20 hours later by Western blot analysis. *$p < 0.05$; **$p < 0.01$; #$p < 0.05$ (vs. RAP alone).

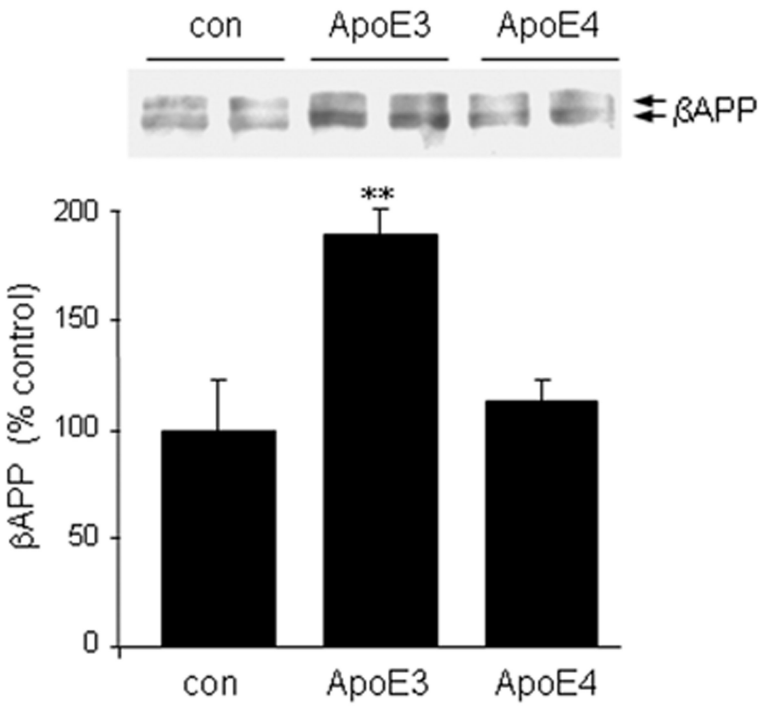

Figure 9.

ApoE directly elevates βAPP expression in an isoform-specific manner. Mouse primary cortical neurons were treated for 20 hours with 5 μg/ml ApoE3 or ApoE4. βAPP levels were then assessed by Western blot analysis. Values represent the mean ± SEM of triplicate determinations. **p < 0.01 vs. control or ApoE4.

J Neuropathol Exp Neurol. Author manuscript; available in PMC 2012 April 24.

Table 1

Patients

	Sex	Race	Age	ApoE genotype	Dementia	Cause of Death	Analysis
1	M	AfrAm	29	3,3	N	thromboembolus	Fig. 1B
2	M	AfrAm	29	3,3	N	osteosarcoma	Fig. 1B
3	M	AfrAm	46	3,3	N	acute myocardial infarction	Fig. 1
4	M	Cauc	50	3,3	N	malignant melanoma	Fig. 1
5	M	Cauc	50	3,3	N	metastatic chondrosarcoma	Fig. 1
6	M	Cauc	72	3,3	N	acute myocardial infarction	Fig. 1
7	M	Cauc	80	3,4	N	lung carcinoma	Fig. 1
8	M	Cauc	81	3,3	N	squamous cell carcinoma	Figs. 1, 4
9	M	AfrAm	77	3,3	N	chronic obstructive pulmonary dis.	Fig. 3A
10	M	Cauc	69	3,3	N	multiorgan failure	Fig. 3
11	M	Cauc	68	3,3	N	pulmonary emboli	Fig. 3
12	M	Cauc	72	3,3	N	acute myocardial infarction	Figs. 3, 4
13	M	Cauc	78	3,3	N	squamous cell carcinoma	Fig. 3B
14	M	Cauc	69	3,3	N	pulmonary emboli	Fig. 3B
15	M	Cauc	78	3,3	N	lung carcinoma	Fig. 4
16	M	Cauc	81	3,3	N	carcinoma of the mouth	Fig. 4
17	M	Cauc	68	3,3	N	pulmonary emboli	Fig. 4
18	M	Cauc	77	n.d.	N[1]	n.d.	Fig. 4
19	F	Cauc	81	n.d.	N[1]	n.d.	Fig. 4
20	M	AfrAm	90	2,4	N[1]	pneumonia	Fig. 4
21	F	Cauc	78	3,4	Y	acute subdural hematoma	Fig. 3
22	F	Cauc	88	3,4	Y	AD complications	Fig. 3
23	M	AfrAm	80	3,3	Y	AD complications	Fig. 3
24	M	Cauc	68	3,3	Y	AD complications	Fig. 3
25	F	Cauc	83	3,4	Y	AD complications	Fig. 3A
26	F	Cauc	69	3,3	Y	AD complications	Fig. 3

	Sex	Race	Age	ApoE genotype	Dementia	Cause of Death	Analysis
27	F	Cauc	88	3,3	Y	AD complications	Fig. 3B
28	F	Cauc	90	3,4	Y	AD complications	Fig. 4
29	M	Cauc	79	3,3	Y	Lung cancer	Fig. 4
30	M	Cauc	68	4,4	Y	AD complications	Fig. 4
31	M	Cauc	71	4,4	Y	myocardial infarction, pneumonia	Fig. 4
32	F	Cauc	88	3,4	Y	AD complications	Fig. 4

[1] Although not clinically demented, these patients showed levels of AD-related pathology consistent with a diagnosis of AD.

Table 2

Summary of AD and Control Subjects[1]

Diagnosis	Age, years (mean ± SD)	Race (% white[2])	Sex (% male)	PMI, hours (mean ± SD)	ApoE (% ε4[3])	Braak&Braak (mean ± SD)
Control	73.4 ± 5.19	85.7	100	12.6 ± 5.71	0	0.4 ± 0.6
AD	79.1 ± 8.17	85.7	28.6[4]	11.2 ± 9.43	21.4	5.1 ± 1.1

[1] These subjects contributed to the data analysis appearing in Figure 3.

[2] Remainder African-American, no Hispanics.

[3] Percent of total alleles (14 per group); remainder ε3, no ε2.

[4] There was no trend towards sex-dependent differences in ApoE or βAPP levels.